

Evidence for Additional Third-Order Transitions in the Two-Dimensional Ising Model

Kedkanok Sitarachu* and Michael Bachmann†

*Soft Matter Systems Research Group, Center for Simulation Physics,
Department of Physics and Astronomy, University of Georgia, Athens, GA 30602, USA*

We employ the microcanonical inflection-point analysis method, developed for the systematic identification and classification of phase transitions in systems of any size, to study the two-dimensional Ising model at various lattice sizes and in the thermodynamic limit. Exact results for the density of states, which were obtained by exact algorithmic computation, provide evidence for higher-order transitions in addition to the well-studied second-order ferromagnetic-paramagnetic phase transition. An independent third-order phase transition is identified in the ferromagnetic phase, whereas another third-order transition resides in the paramagnetic phase. The latter is a dependent transition, i.e., it is inevitably associated with the critical transition, but it remains separate from the critical point in the thermodynamic limit. For a deeper insight into the nature of these additional transitions, a detailed analysis of spin clusters is performed.

I. INTRODUCTION

The (Lenz-)Ising model was introduced about a century ago for studies of the impacts of attractive local spin-spin interaction upon macroscopic cooperative ordering across the entire system [1, 2]. As it turned out, the one-dimensional spin chain does not exhibit signs of a thermodynamic phase transition. It took almost two decades to solve the two-dimensional problem and to reveal the prominent second-order phase transition that separates the paramagnetic and the ferromagnetic phase [3, 4]. In the following decades, the simplicity and versatility of the model, an increased interest in understanding the origins of phase transitions, and the ever growing available computer power made the Ising model one of the most widely employed generic models for studies of complexity.

Traditional theory dictates that phase transitions can only occur in the thermodynamic limit, which is where energetic and configurational response parameters tend to exhibit nonanalyticities at the transition point. From a modern point of view, this strict definition was mostly a reference to the mathematical tractability of complex problems. For the same reason, most studies of phase transitions were performed by employing canonical statistical analysis techniques. However, this approach is known to lead to problems in interpreting signals in response functions for systems of finite size. With fields like nano- and biosciences moving into the focus of statistical analysis, where cooperative system behavior is governed or at least strongly influenced by finite-size effects, the theory of phase transitions has to be extended and statistical analysis techniques appropriately adapted.

The significant evolution of computational resources throughout the last decades now allows algorithmic access to problems where a mathematical approach is not

manageable. As desirable a rigorous treatment is, computational methods offer additional options for estimating or calculating quantities that are virtually inaccessible mathematically. One of the most interesting such quantity is the number (or density) $g(E)$ of microstates with system energy E . The logarithm of the density of states is commonly interpreted as the microcanonical entropy [5]

$$S(E) = k_B \ln g(E). \quad (1)$$

The generalized microcanonical inflection-point analysis method was introduced for the study of systems of any size [6]. It rests on the principle of minimal sensitivity [7, 8] in the interplay between the configurational entropy $S(E)$ and the system energy E . In the microcanonical theory of phase transitions, these are considered the central quantities that govern effects competing with each other for dominance in the respective phases [5, 9]. In consequence, their balance ensures a stable equilibrium state. In our method, the entropy and its derivatives with respect to energy are systematically analyzed to identify and classify transition signals uniquely [6]. The idea is similar to Ehrenfest's approach to identifying and classifying phase transitions by means of nonanalyticities in derivatives of thermodynamic potentials [10]. However, the Ehrenfest scheme cannot be systematically extended to accommodate finite systems as nonanalyticities can only occur in the (hypothetical) thermodynamic limit.

We recently employed our method to analyze the phase behavior of various Ising systems [6, 11, 12]. As expected, the inflection-point analysis did not reveal transition signatures for the one-dimensional Ising chain. However, Ising strips and the two-dimensional (2D) Ising model on the square lattice exhibit a variety of transition signals. Particularly interesting are the higher-order transitions we found for the 2D Ising model in addition to the well-studied critical transition. According to our classification scheme, the critical transition is a second-order *independent* transition, whereas an additional *dependent* third-order transition was identified in the paramagnetic phase

* E-mail: Kedkanok.Sitarachu@uga.edu

† E-mail: bachmann@smsyslab.org;

Homepage: <http://www.smsyslab.org>

that is inevitably linked to the critical transition. It can be interpreted as the precursor of the critical transition in the disordered phase. Another independent transition is located in the ordered phase. In this paper, we provide evidence that these two additional transitions remain separate from the critical transition in the thermodynamic limit and thus can be considered phase transitions in the more general context provided by the microcanonical theory. By performing a detailed analysis of spin clusters, we also shed light on the character of these additional transitions.

It is worth noting that the microcanonical inflection-point analysis method has not only been successfully employed for spin systems, but also in studies of macromolecular systems [6, 13, 14]. It has proven useful as a foundation for a better understanding of general geometric properties of phase transitions [15, 16] as well.

The paper is organized as follows: The Ising model, computational techniques, and the microcanonical analysis method are briefly reviewed in Section II. Results obtained by microcanonical inflection-point analysis are presented in Section III. Properties of the additional transitions identified by means of spin-cluster analyses are discussed in Section IV. The summary of the major results in Section V concludes the paper.

II. MICROCANONICAL STATISTICAL ANALYSIS AND CLUSTER SIMULATIONS OF THE 2D ISING MODEL

In the following, we briefly review the Ising model, the microcanonical inflection-point analysis method, and the simulation methodology used for the cluster analysis.

A. Ising model

In the two-dimensional Ising model [1, 2] with periodic boundary conditions and absent external magnetic field, the energy of the spin configuration $\mathbf{X} = (s_1, s_2, \dots, s_N)$ with $N = L \times L$ spins on a square lattice with edge lengths L can simply be written as

$$E(\mathbf{X}) = -J \sum_{\langle i, j \rangle} s_i s_j. \quad (2)$$

Possible values of the spin orientation are $s_{i,j} = \pm 1$. The symbol $\langle i, j \rangle$ indicates that only interactions of the spins s_i and s_j are considered, if they are nearest neighbors on the lattice. The energy scale is fixed by the positive-valued coupling constant $J > 0$ (ferromagnetic coupling).

B. Microcanonical inflection-point analysis method

The microcanonical inflection-point analysis method, which utilizes the principle of least sensitivity [7, 8], was

introduced to systematically identify and classify transition signals in systems of any size [6]. Like in canonical statistical analysis, the general assumption is that the interplay of entropy and energy governs the transition behavior.

In our method, least-sensitive inflection points of $S(E)$, as defined in Eq. (1), and its derivatives are used to identify phase transitions. We denote the derivatives as follows: $\beta(E) = dS(E)/dE$, $\gamma(E) = d^2S(E)/dE^2$, and $\delta(E) = d^3S(E)/dE^3$. Derivatives of higher order were not considered in this study.

As it turns out, it is useful to distinguish two types of transitions. *Independent* transitions are analogs of the conventional transitions and their occurrence does not depend on other cooperative processes in the system. This is in contrast to *dependent* transitions, which are inevitably associated with an independent transition. These transitions only occur at a higher energy (i.e., usually in the less-ordered phase), and they are of higher order than the corresponding independent transition. Therefore, dependent transitions can be considered precursors of a major independent transitions. This may have noticeable consequences for applications: If a system currently in the disordered phase is adiabatically cooled down and a dependent transition signal is detected, a major phase transition is imminent upon further cooling.

Independent transitions are classified as of odd order $(2n-1)$, where n is positive integer, if the inflection point at transition energy E_{tr} satisfies the condition

$$\left. \frac{d^{(2n-1)}S(E)}{dE^{(2n-1)}} \right|_{E=E_{tr}} > 0, \quad (3)$$

whereas for even-order $(2n)$ independent transitions

$$\left. \frac{d^{2n}S(E)}{dE^{2n}} \right|_{E=E_{tr}} < 0 \quad (4)$$

holds. Inflection points are associated with even-order $(2n)$ *dependent* transitions, if

$$\left. \frac{d^{2n}S(E)}{dE^{2n}} \right|_{E=E_{tr}} > 0, \quad (5)$$

and odd-order $(2n+1)$ dependent transitions are characterized by

$$\left. \frac{d^{(2n+1)}S(E)}{dE^{(2n+1)}} \right|_{E=E_{tr}} < 0. \quad (6)$$

For finite 2D Ising systems, it is convenient to use the exact algorithmic evaluation schemes introduced in Refs. [17, 18] to determine the density of states. The latter method also allows for an extrapolation toward the thermodynamic limit, which will eventually permit us to decide whether or not transitions identified by means of the inflection-point method will survive in this limit. The derivatives of the microcanonical entropy are then obtained by numerical differentiation [12].

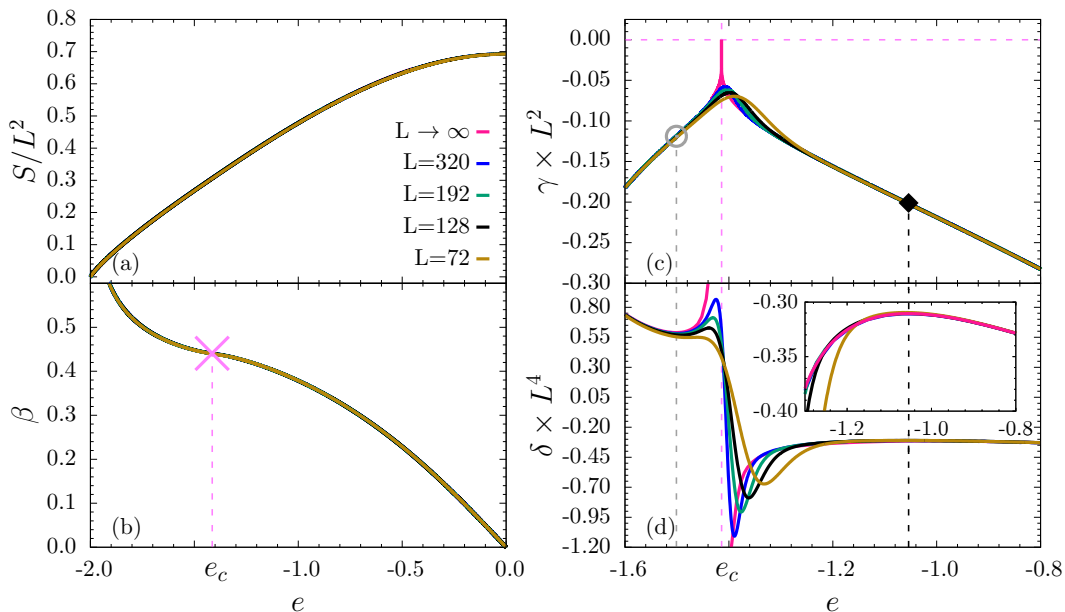


FIG. 1. (a) Microcanonical entropy per spin $S(e)/L^2$ and its derivatives (b) $\beta(e)$, (c) $\gamma(e)L^2$, and (d) $\delta(e)L^4$ for various system sizes, plotted as functions of the energy per spin $e = E/L^2$. The dashed vertical lines mark the transition energies per spin associated with the three transitions found in the 2D Ising model. For reference, the critical energy per spin is $e_c \approx -1.414$.

C. Wolff cluster algorithm

For the study of cluster properties of the Ising system, we employed the Wolff single-cluster algorithm [19]. Instead of performing single spin-flip Monte Carlo updates, in this method an entire cluster of spins is updated in a single step. This is most efficient near the critical point and in the subcritical ferromagnetic region, where the majority cluster coexists with smaller minority clusters.

In this simple yet powerful Monte Carlo method, one spin in the system is selected randomly. Then, nearest-neighbor spins with the same orientation are identified and added to the (stochastic) Wolff cluster with probability $p = 1 - \exp(-2\beta J)$, where $\beta = 1/k_B T$ is the inverse thermal energy at temperature T (the Boltzmann constant k_B was set to unity in the simulations and in the subsequent analysis). The process of adding spins to the Wolff cluster is repeated until all spins belonging to the same geometric cluster have been tested and the construction of the Wolff cluster is complete. Eventually, all spins in this cluster are flipped. For the identification of a geometric cluster, we used the standard labeling technique introduced by Hoshen and Kopelman [20].

III. TRANSITION SIGNALS FROM MICROCANONICAL ANALYSIS

Exact algorithmic methods [17, 18] were employed to determine the densities of states of the 2D Ising model with periodic boundary conditions for lattice sizes with up to 320×320 spins. The method by Häggkvist et al. [18]

also allows to find the density of states in the thermodynamic limit ($L \rightarrow \infty$), which is key to judging whether or not the additional third-order transitions predicted previously [6, 11, 12] survive in this limit. Based on the exact data obtained from these algorithms, the microcanonical inflection-point analysis method was then used to identify transitions in the curves of the microcanonical entropy and its derivatives.

The microcanonical results are shown in Fig. 1. The quantities are properly rescaled to account for obvious system size dependence and plotted as functions of the energy per spin, $e = E/L^2$. Rescaled entropy and β curves in Fig. 1(a) and 1(b), respectively, do not exhibit much system size dependence on the scales plotted. However, whereas there is no inflection point in the entropy, the β curves do possess a unique least-sensitive inflection point, which indicates the well-studied critical transition separating the ferromagnetic from the paramagnetic phase. According to our microcanonical classification scheme, it satisfies the criteria of an *independent* second-order phase transition. In the thermodynamic limit, the critical transition energy per spin is $e_c \approx -1.414$ and the critical temperature coincides with Onsager's result: $T_c = 2/\ln(1 + \sqrt{2}) \equiv 1/\beta(e_c) \approx 2.269$, as expected. Towards the thermodynamic limit ($L \rightarrow \infty$), the slope converges to zero, as can clearly be seen in the next derivative $\gamma(E)$, shown in Fig. 1(c). Interestingly, the smooth peak visible for finite systems turns into a cusp in the thermodynamic limit. Consequently, the nondifferentiability of γ at the critical transition energy leads to a discontinuity in the next-higher derivative δ [Fig. 1(d)].

In addition to the critical transition, the microcanonical inflection-point analysis method identifies two addi-

tional transitions of higher order. An *independent* third-order transition (fourth order for $L \leq 64$) is identified in the ferromagnetic phase. The corresponding least-sensitive inflection point in γ [Fig. 1(c)] leads to a pronounced positive-valued local minimum in $\delta(e)$. In the thermodynamic limit, the transition energy is $e_{\text{ind}} \approx -1.502$, which corresponds to the transition temperature $T_{\text{ind}} \approx 2.229$.

Equally interesting is the occurrence of the *dependent* third-order transition in the paramagnetic phase. As it is inevitably coupled to the critical transition, it can be imagined as a precursor of this major transition in the disordered phase. The least-sensitive inflection point in $\gamma(e)$, which converges to the transition energy $e_{\text{dep}} = -1.053$ (corresponding to the transition temperature $T_{\text{dep}} = 2.567$) in the thermodynamic limit, is characterized by a negative-valued peak in δ . The inset in Fig. 1(d) shows that this peak is also present in thermodynamic limit.

Whereas these additional transitions do not exhibit nonanalytic features in the way the critical transition does, the distinct signals indicating their existence survive in the thermodynamic limit and do not converge toward the critical point. This is a remarkable result as the subphases between them and the critical point create an “atmosphere” surrounding the critical transition. The dependent transition may potentially provide additional clues as to the loss of identity in the system when it approaches the critical point upon cooling. However, it is important to emphasize that the third-order transition in the ferromagnetic phase is independent of the critical transition and thus does not necessarily help understanding better the approach toward the critical transition upon adiabatic heating. It does not serve as a precursor of it in the way the dependent transition in the paramagnetic phase does.

Figure 2 contains the results for the transition temperatures obtained by microcanonical analysis for various lattice sizes and in the thermodynamic limit (dashed lines). It is important to note that the additional third-order transitions neither disappear nor converge toward the critical point in the thermodynamic limit. The transition temperatures remain well-separated from the critical temperature, but the microcanonical transition features do not develop into non-analyticities. Hence, these transitions are not phase transitions in the conventional Ehrenfest scheme. However, it should be reiterated that significant changes in system behavior in modern scientific problems and industrial applications – for many of which the thermodynamic limit is a nonsensical simplification – are not signaled by catastrophic changes in observables and data, but are rather subtle. Processes like folding and aggregation transitions of macromolecules, weather phenomena, swarm formation, and even synchronization in computer networks and social behavior occur on mesoscopic rather than macroscopic length scales. In fact, the early detection of sublying patterns leading to a catastrophic event may be more important and revealing

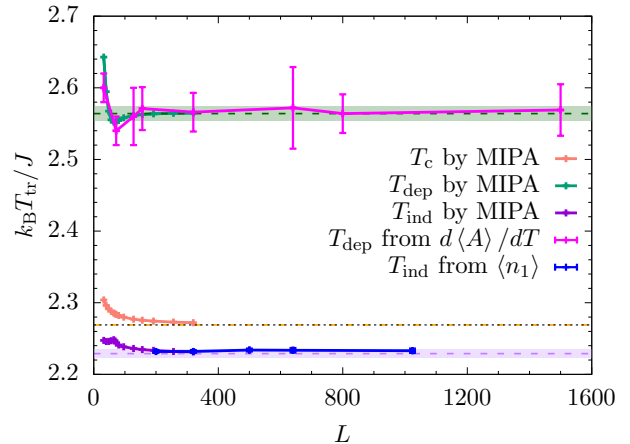


FIG. 2. Transition temperatures T_{tr} obtained by microcanonical inflection-point analysis (MIPA) and cluster properties plotted as a function of L . Symbols mark the transition temperatures at finite system size (solid lines are only guides to the eye). Horizontal dashed lines are located at the transition temperatures in the thermodynamic limit ($L \rightarrow \infty$) found by microcanonical analysis. For reference, the critical temperature is $k_B T_c / J = 2 / \ln(1 + \sqrt{2}) \approx 2.269$. The small uncertainties in the microcanonical results originate from the numerical error in locating the transition signals due to the necessity of using discrete differences methods for calculating derivatives.

than a thorough study of the major transition itself.

IV. ANALYSIS OF SPIN CLUSTERS

We now discuss the results obtained by Wolff spin-cluster simulations and cluster analysis to shed more light on the system behavior associated with the additional transitions in the Ising model identified by microcanonical inflection-point analysis.

A. Third-order dependent transition in the paramagnetic phase

In order to gain more insight into the nature of the additional third-order transitions identified for the 2D Ising model, cluster simulations were performed and cluster sizes analyzed by means of canonical statistical analyses of suitable order parameters. A typical example of a spin configuration on the square lattice with 1500×1500 with all clusters colored differently is shown in Fig. 3.

The first quantity we take a closer look at is the average cluster size, $\langle A \rangle$. We define A as the average size of clusters containing more than a single spin in a given

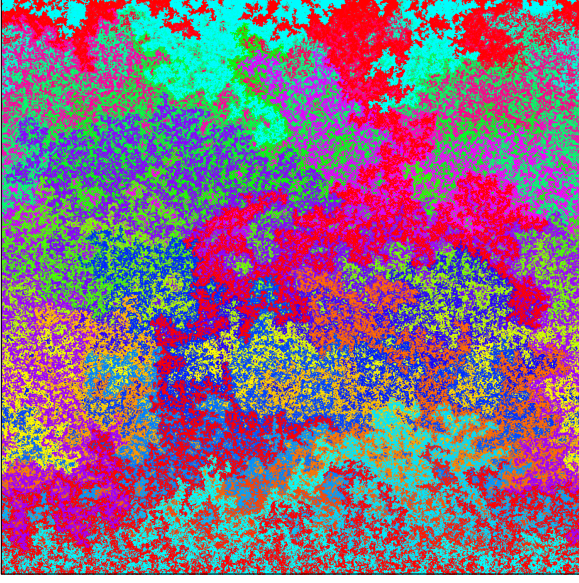


FIG. 3. Clusters identified in a typical spin configuration on the 1500×1500 lattice in the paramagnetic phase at $T = 2.605$, which is just above the dependent-transition point $T_{\text{dep}} \approx 2.567$.

spin configuration \mathbf{X} :

$$A = \frac{1}{n'} \sum_{l'} C_{l'}, \quad (7)$$

where l' labels the clusters with more than one spin, $C_{l'}$ is the number of spins in cluster l' , and n' is the total number of clusters with more than one spin in \mathbf{X} . The statistical average is then obtained as

$$\langle A \rangle = \frac{1}{Z} \sum_{\mathbf{X}} A(\mathbf{X}) e^{-E(\mathbf{X})/k_B T}, \quad (8)$$

where T is the canonical temperature and $Z = \sum_{\mathbf{X}} \exp[-E(\mathbf{X})/k_B T]$ is the canonical partition function.

As mentioned, spin configurations at different temperatures were obtained in Wolff cluster simulations [19]. At each temperature, up to 10^8 spin configurations were generated. Spin clusters were labeled by means of the Hoshen-Kopelman method [20] and the average cluster size A in a given configuration was determined. The canonical average of this quantity and its derivative with respect to the temperature are plotted as functions of the temperature for various lattice sizes in Fig. 4.

Figure 4(a) shows that at low temperatures, in the ferromagnetic phase, the average cluster size decreases with increasing temperatures. Near the critical temperature, $\langle A \rangle$ exhibits a backbending pattern, which becomes more pronounced for larger lattices. For temperatures $T > T_c$, i.e., in the paramagnetic phase, the average cluster size decreases again. The temperature derivative of the average cluster size, $d\langle A \rangle/dT$, is shown in Fig. 4(b). It is

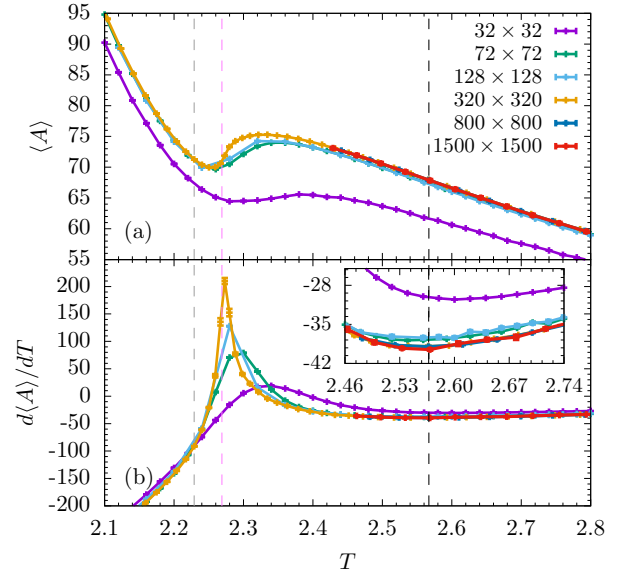


FIG. 4. (a) Average cluster size $\langle A \rangle$ and (b) derivative $d\langle A \rangle/dT$ as functions of temperature T for the two-dimensional Ising model at various system sizes. The inset enlarges the area surrounding the dependent third-order transition in the paramagnetic phase. Note that cluster simulations for system sizes 800×800 and 1500×1500 were only performed for temperatures $T \geq 2.46$. The black dashed line indicates the location of the dependent third-order transition in the thermodynamic limit as obtained from microcanonical analysis, $T_{\text{dep}} \approx 2.567$. The other dashed lines locate the critical second-order and the subcritical independent third-order transition, respectively.

a measure for the rate of change of the average cluster size with respect to the temperature. The curves for the different system sizes all show a prominent peak associated with the inflection point in the backbending pattern in Fig. 4(a). The peak location converges to the critical point, as expected. As a thermodynamic response quantity, it eventually becomes nonanalytic at the critical point in the thermodynamic limit.

More interesting is the inflection point of $\langle A \rangle$ in the paramagnetic phase close to the dependent third-order transition identified by microcanonical analysis. It does not disappear even for the largest lattices simulated (1500×1500). The curves of the derivative $d\langle A \rangle/dT$ exhibit a local minimum and there is no indication for it to flatten out in the thermodynamic limit. Its close proximity to the transition temperature of the dependent third-order transition $T_{\text{dep}} \approx 2.567$ suggests that this feature is related to the transition.

The decrease of the average cluster size with increasing temperature is expected in the paramagnetic phase. However, it is noteworthy that this decrease accelerates for temperatures $T < T_{\text{dep}}$, before slowing down for $T > T_{\text{dep}}$. This is an unexpected system behavior; the average cluster size could simply drop monotonously in the paramagnetic phase (in which case the third-order de-

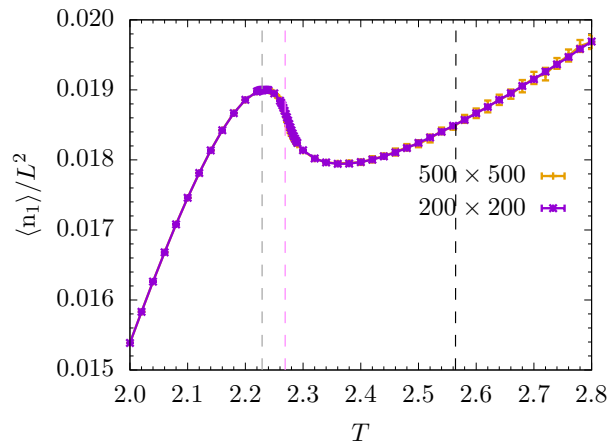


FIG. 5. Average number of isolated spins per spin, $\langle n_1 \rangle$, as a function of temperature for two lattice sizes. Vertical dashed lines are located at the transition temperatures of the 2D Ising model obtained by microcanonical analysis.

pendent transition would not exist). Although it seems to be a minor effect, this change of monotony is, in fact, an important signature of the catastrophic critical transition, because, as we have shown in the microcanonical analysis, these transitions are inevitably associated with each other. This means that the third-order dependent transition is a precursor of the critical transition in the paramagnetic phase, and – as our results from the cluster analysis show – is due to the change of the rate by which clusters decay in the disordered phase.

The estimates for the peak temperatures in $d\langle A \rangle / dT$ in the paramagnetic phase have already been included in Fig. 2. They clearly converge to the third-order dependent transition temperature obtained by microcanonical analysis in the thermodynamic limit. Even for the finite lattices, the respective microcanonical estimate and the estimate from the cluster analysis are very close to each other, suggesting that the third-order transition signaled by microcanonical analysis is indeed due to the enhanced fluctuations about the average cluster size in this temperature region.

B. Third-order independent transition in the ferromagnetic phase

For the study of properties of the third-order independent transition in the ordered (ferromagnetic) phase, we look at signs of emerging disorder and entropic variability, which is dependent on the formation of minority clusters in this phase, where the ferromagnetic states are always dominated by a majority cluster. The simplest of these is obviously what we call the “single-spin cluster”, i.e., an isolated single spin surrounded by nearest-neighbor spins with opposite orientation. Figure 5 shows plots of the statistical average of the number of isolated spins $\langle n_1 \rangle$ as a function of temperature for two different

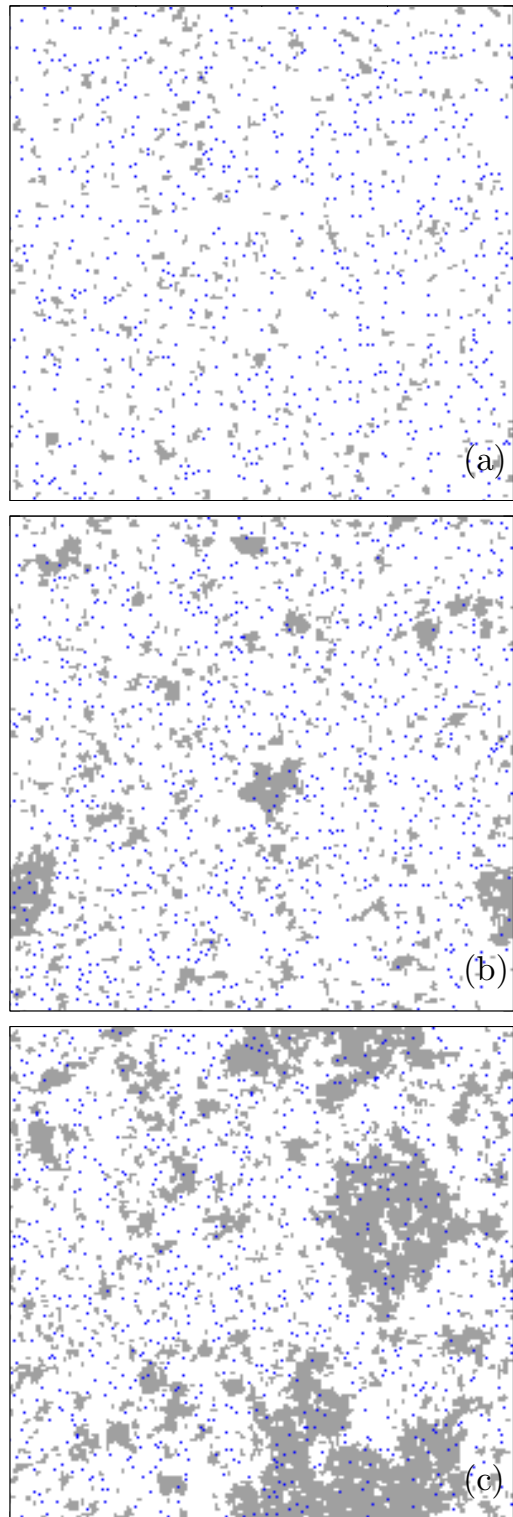


FIG. 6. Representative Ising configurations on the 200×200 lattice at (a) $T = 2.10$, (b) $T = 2.23$, and (c) $T = 2.28$. In white areas, spins point up and in grey areas down. Isolated spins, independent of their orientation, are colored blue. The numbers of isolated spins divided by the total number of spins, n_1 , are: (a) 0.0169, (b) 0.0197, and (c) 0.0179.

lattice sizes. These results were also obtained in Wolff cluster simulations. Dashed vertical lines mark the transition points found by microcanonical analysis.

Most noteworthy is the peak near the third-order independent transition temperature $T_{\text{ind}} \approx 2.229$ in the ferromagnetic phase and the subsequent drop toward the critical point. As expected, the number of isolated spins increases again with temperature in the paramagnetic phase.

The drop in the number of isolated spins in the ferromagnetic phase just below the critical point can be attributed to the dissolution of the majority cluster. Isolated spins serve as “bond breakers.” Their increased numbers and the subsequent recombination into clusters of smaller size with more and more rugged fractal boundaries occur near the third-order transition temperature. These cluster structures are not present in the pure ferromagnetic phase below T_{ind} . In fact, clusters of intermediate size do not exist at all.

For example, an analysis of cluster sizes for the 500×500 lattice revealed that near T_{ind} clusters of sizes in the range 10%–70% of the system size are completely absent. The population of intermediate-size cluster rapidly increases toward the critical temperature, though. The isolated spins help seed the formation of these clusters. Representative configurations on the 200×200 Ising lattice are shown in Fig. 6 for temperatures (a) below T_{ind} , (b) near T_{ind} , and (c) close to T_c . Note that the transition at $T_{\text{int}} \approx 2.229$ is an independent transition, i.e., it is not associated with the critical transition.

In Fig. 2, we have already included the transition temperatures of this transition for various lattice sizes. Even for the largest system simulated in this phase, 1024×1024 spins, the peak temperature read off from $\langle n_1 \rangle$ is very close to the microcanonical estimate at this system size. Most importantly, the transition temperature estimates for 1024×1024 and even smaller lattice sizes, are located well within the narrow uncertainty region of the microcanonical estimate for the transition temperature in the thermodynamic limit. This increases the confidence that the peaking in the average number of isolated spins in the ferromagnetic phase is a major feature of the system behavior in the vicinity of this third-order transition. As expected, the finite-size transition temperatures of this additional transition do not converge toward the critical temperature, but remain separate from the critical point even in the thermodynamic limit.

V. SUMMARY

The purpose of this study was twofold: First, it was necessary to verify that the recently found additional phase transitions in the two-dimensional Ising model flanking the critical transition remain present and well-separated from the critical transition in the thermodynamic limit. This goal could be achieved by microcanonical inflection-point analysis of the microcanonical entropy and the relevant derivatives [6] in the thermodynamic limit. This was made possible by means of the exact enumeration method for the density of states of the Ising model introduced by Häggkvist et al. [18].

The second objective was to find evidence of the third-order transitions in the way the Ising system forms clusters in both the paramagnetic and the ferromagnetic phase. For this purpose, extensive Wolff single-cluster simulations [19] for lattice systems with up to 1500×1500 spins were performed and suitably introduced order parameters measured.

It turned out that the fluctuations of the average cluster size (excluding isolated single spins) become extremal at about the temperature of the third-order dependent transition in the paramagnetic phase. This suggests that a collective pre-ordering of spins occurs in this temperature region in the disordered phase as a precursor of the critical transition.

In the ferromagnetic phase, the average number of isolated spins peaks at the independent third-order transition temperature that was identified by microcanonical analysis. Here, the increased number of such “seeds” of disorder in the ferromagnetic phase enables the formation of critical clusters once the critical point is approached.

These results are encouraging and may initiate a search for higher-order transitions in other systems as well. Our analysis also shows that the study of sublying transitions in ordered and disordered phases can lead to a better understanding of the system-inherent reasons leading to major phase transitions. Dependent transitions, which are inevitably coupled to a major transition, are precursors of imminent global ordering processes in the disordered phase. The understanding of such precursor transitions may aid predicting significant ordering effects such as cooperativity and synchronization in complex systems before they actually happen.

ACKNOWLEDGMENTS

We thank the Georgia Advanced Computing Resource Center (GACRC) at the University of Georgia for providing computational resources.

-
- [1] W. Lenz, Z. Phys. **21**, 613 (1920).
 - [2] E. Ising, Z. Phys. **31**, 253 (1925).

- [3] L. Onsager, Phys. Rev. **65**, 117 (1944).
- [4] B. Kaufman, Phys. Rev. **76**, 1232 (1949).

- [5] D. H. E. Gross, *Microcanonical Thermodynamics* (World Scientific, Singapore, 2001).
- [6] K. Qi and M. Bachmann, Phys. Rev. Lett. **120**, 180601 (2018).
- [7] P. M. Stevenson, Phys. Rev. D **23**, 2916 (1981).
- [8] P. M. Stevenson, Phys. Lett. B **100**, 61 (1981).
- [9] M. Bachmann, *Thermodynamics and Statistical Mechanics of Macromolecular Systems* (Cambridge University Press, Cambridge UK, 2014).
- [10] P. Ehrenfest, Proc. Royal Acad. Amsterdam (Netherlands) **36**, 153 (1933); Commun. Kamerlingh Onnes Inst. Leiden Suppl. No. 75b.
- [11] K. Sitarachu and M. Bachmann, J. Phys. Conf. Ser. **1483**, 012009 (2020).
- [12] K. Sitarachu, R. K. P. Zia, and M. Bachmann, J. Stat. Mech. (JSTAT), **2020**, 073204 (2020).
- [13] D. Aierken and M. Bachmann, Polymers **12**, 3013 (2020).
- [14] L.F. Trugilho and L.G. Rizzi, J. Stat. Phys. **186**, 40 (2022).
- [15] G. Pettini, M. Gori, R. Franzosi, C. Clementi, and M. Pettini, Physica A **516**, 376-392 (2019).
- [16] G. Bel-Hadj-Aissa, M. Gori, V. Penna, G. Pettini, and R. Franzosi, Entropy **22**, 380 (2020).
- [17] P. D. Beale, Phys. Rev. Lett. **76**, 78 (1996).
- [18] R. Häggkvist, A. Rosengren, D. Andrén, P. Kundrotas, P. H. Lundow, and K. Markström, Phys. Rev. E **69**, 046104 (2004).
- [19] U. Wolff, Phys. Rev. Lett. **62**, 361 (1989).
- [20] J. Hoshen and R. Kopelman, Phys. Rev. B **14**, 3438 (1976).